



## Novel esophageal squamous cell carcinoma bone metastatic clone isolated by scintigraphy, X ray and micro PET/CT

Bi-Zeng Zhao, Jie Cao, Jin-Chen Shao, Yan-Bing Sun, Li-Min Fan, Chun-Yu Wu, Sheng Liang, Bao-Feng Guo, Guang Yang, Wen-Hui Xie, Qing-Cheng Yang, Shun-Fang Yang

Bi-Zeng Zhao, Qing-Cheng Yang, Department of Orthopedics, Shanghai Sixth Hospital of Shanghai Jiaotong University, Shanghai 200233, China

Jie Cao, Wen-Hui Xie, Shun-Fang Yang, Department of Nuclear Medicine, Shanghai Chest Hospital of Shanghai Jiaotong University, Shanghai 200030, China

Jin-Chen Shao, Department of Pathology, Shanghai Chest Hospital of Shanghai Jiaotong University, Shanghai 200030, China

Yan-Bing Sun, Department of Radiology, Shanghai Chest Hospital of Shanghai Jiaotong University, Shanghai 200030, China

Li-Min Fan, Department of Thoracic Surgery, Shanghai Chest Hospital of Shanghai Jiaotong University, Shanghai 200030, China

Chun-Yu Wu, Bao-Feng Guo, Department of Breast Surgery, Shanghai Long Hua Hospital of Shanghai University of Traditional Chinese Medicine, Shanghai 200032, China

Sheng Liang, Micro PET/CT Center, Department of Nuclear Medicine, Shanghai RuiJin Hospital of Shanghai Jiaotong University, Shanghai 200025, China

Guang Yang, Kyocera Communication Systems (Shanghai) Co., Ltd, Shanghai 201203, China

**Author contributions:** Zhao BZ and Fan LM were responsible for animal experiments and collection of human specimens; Cao J and Xie WH contributed to the tail vein injection of radionuclide and pinhole bone scintigraphy; Yang QC participated in experimental design; Shao JC contributed to pathological diagnosis; Sun YB contributed to human conventional radiography used in the mice; Wu CY and Guo BF contributed to statistical analysis and real-time polymerase chain reaction; Liang S contributed to micro positron emission/computed tomography; Yang G contributed to images processing; Yang SF designed the study and wrote the manuscript; all authors read and approved the final version.

**Supported by** Shanghai Science and Technology fundamental research Grant 08140902202 and 09140901500 (to Yang SF); and National Natural Science Foundation of China Grant 30973017 (to Yang QC)

**Correspondence to:** Yang Shun-Fang, Associate Professor, Department of Nuclear Medicine, Shanghai Chest Hospital, Shanghai Jiaotong University, Shanghai 200030, China. [yzyg@sh163.net](mailto:yzyg@sh163.net)

Telephone: +86-21-62821990 Fax: +86-21-62801109;

Received: April 24, 2013 Revised: September 21, 2013

Accepted: September 29, 2013

Published online: January 28, 2014

### Abstract

**AIM:** To establish a Chinese esophageal squamous cell carcinoma (ESCC) cell line with high bone metastasis potency using  $^{99m}\text{Tc}$ -methylene diphosphonate ( $^{99m}\text{Tc}$ -MDP) micro-pinhole scintigraphy, X ray and micro-positron emission tomography/computed tomography (PET/CT) for exploring the mechanism of occurrence and development in esophageal cancer.

**METHODS:** The cells came from a BALB/c nu/nu immunodeficient mouse, and oncogenic tumor tissue was from a surgical specimen from a 61-year-old male patient with ESCC. The cell growth curve was mapped and analysis of chromosome karyotype was performed. Approximately  $1 \times 10^6$  oncogenic cells were injected into the left cardiac ventricle of immunodeficient mice. The bone metastatic lesions of tumor-bearing mice were detected by  $^{99m}\text{Tc}$ -MDP scintigraphy, micro-PET/CT and X-ray, and were resected from the mice under deep anesthesia. The bone metastatic cells in the lesions were used for culture and for repeated intracardiac inoculation. This *in vivo/in vitro* experimental metastasis study was repeated for four cycles. All of the suspicious bone sites were confirmed by pathology. Real-time polymerase chain reaction was used to compare the gene expression in the parental cells and in the bone metastatic clone.

**RESULTS:** The surgical specimen was implanted subcutaneously in immunodeficient mice and the tumorigenesis rate was 100%. First-passage oncogenic cells were named CEK-Sq-1. The chromosome karyotype analysis of the cell line was hypotriploid. The bone

metastasis rate went from 20% with the first-passage oncogenic cells *via* intracardiac inoculation to 90% after four cycles. The established bone metastasis clone named CEK-Sq-1BM had a high potential to metastasize in bone, including mandible, humerus, thoracic and lumbar vertebrae, scapula and femur. The bone metastasis lesions were successfully detected by micro-pinhole bone scintigraphy, micro-PET/CT, and X-ray. The sensitivity, specificity and accuracy of the micro-pinhole scintigraphy, X-ray, and micro-PET/CT imaging examinations were: 89.66%/32%/80%, 88.2%/100%/89.2%, and 88.75%/77.5%/87.5%, respectively. Some gene expression difference was found between parental and bone metastasis cells.

**CONCLUSION:** This newly established Chinese ESCC cell line and animal model may provide a useful tool for the study of the pathogenesis and development of esophageal carcinoma.

© 2014 Baishideng Publishing Group Co., Limited. All rights reserved.

**Key words:** Esophageal squamous cell carcinoma; Cell line; Bone metastasis; Molecular imaging; Real-time polymerase chain reaction

**Core tip:** We established a novel esophageal squamous cell carcinoma cell line from a surgically resected human specimen and its clone with mixed bone metastasis potency by molecular imaging including conventional radiography, bone scintigraphy, and micro-positron emission tomography/computed tomography after intracardiac inoculation of the cells into nude mice. The process was repeated *in vivo* and *in vitro* for four cycles to obtain a bone metastasis clone CEK-Sq-1BM. Some gene expression difference was compared with the primary cells and their clone by real-time reverse transcriptase polymerase chain reaction. This work may be helpful for research in bone metastases.

Zhao BZ, Cao J, Shao JC, Sun YB, Fan LM, Wu CY, Liang S, Guo BF, Yang G, Xie WH, Yang QC, Yang SF. Novel esophageal squamous cell carcinoma bone metastatic clone isolated by scintigraphy, X ray and micro PET/CT. *World J Gastroenterol* 2014; 20(4): 1030-1037 Available from: URL: <http://www.wjgnet.com/1007-9327/full/v20/i4/1030.htm> DOI: <http://dx.doi.org/10.3748/wjg.v20.i4.1030>

## INTRODUCTION

Esophageal cancer (EC) is among the top six leading causes of death from cancer; it exhibits a strikingly uneven geographical distribution, resulting in focal endemic high-incidence areas in several countries<sup>[1]</sup>, including Northern China, Northern Iran and South Africa. Considerable advances in diagnosis, surgical techniques and chemoradiotherapy have been made for EC. Nevertheless, EC remains one of the most lethal cancers and

most patients die from recurrence or metastasis, with a 5-year survival rate as low as 16% in the United States in 1996-2004, and it was ranked fifth among the five leading causes of cancer mortality in male patients aged 40-79 years in 2008<sup>[2,3]</sup>. In China, the situation is even worse<sup>[4]</sup>. The most common metastatic sites of EC are lung, liver and bone. The median survival time is < 1 year for advanced cases. To improve survival for EC patients, a better understanding of the cellular and molecular carcinogenesis of EC, and especially of the mechanism of metastasis, is needed. Well-characterized human EC cell lines and animal models for metastasis are important research resources for studying cancer cell biology, as well as for developing new strategies against EC. Although there are many EC cell lines<sup>[5-9]</sup>, a bone metastasis model is lacking. To enrich the bank of cell lines and animal models of EC, a new human EC cell line (CEK-Sq-1) and its clone with a high bone-seeking tendency were established. Their morphological and biological characteristics and tumorigenicity *in vivo* were described in this experimental study, which may provide a useful model for *in vitro* and *in vivo* cellular and molecular research.

## MATERIALS AND METHODS

With the patient's consent, an esophageal squamous cell carcinoma (ESCC) tumor specimen was surgically removed from a 61-year-old Chinese man. The tumor was diagnosed pathologically as T2N1M0 after surgery. Lymph node metastasis occurred 6 mo later and bone metastasis 1 year after the operation. Fresh tumor tissue specimens were cut into small pieces of about 1 mm<sup>3</sup> and soaked with 40000 U/mL penicillin and 1000 µg/mL streptomycin (Northern China Pharmaceutical, Shijiazhuang, China) for about 5 min.

### Xenograft and cell culture

The specimens were implanted subcutaneously in three immunodeficient mice and the tumorigenesis rate was 100% after 4 wk. The xenograft tumor was excised after the mouse was deeply anesthetized and then sacrificed. The tumor was minced for cell culture in 25-cm<sup>2</sup> culture flasks with 6 mL RPMI 1640 medium (Gibco, Carlsbad, CA, United States) containing 10% fetal bovine serum (Gibco), 100 U/mL penicillin and 100 µg/mL streptomycin (Northern China Pharmaceutical). The cells were cultured at 37 °C in an atmosphere with 5% CO<sub>2</sub>. The first-passage oncogenic cells were cultured after growing for 7 d. The cells were named CEK-Sq-1.

### Chromosome analysis

The CEK-Sq-1 cells at the 15<sup>th</sup> passage at the stage of proliferation were selected and treated with colchicine for 4-6 h. The cell suspension was collected and Giemsa-stained after hypotonic treatment. We selected cells with well-dispersed chromosomes in metaphase. The chromosome distribution and karyotype features were investigated by analyzing 40 and 15 metaphases, respectively.

### Growth characteristics of the cell line

The CEK-Sq-1 cells of the 7<sup>th</sup>, 24<sup>th</sup> and 40<sup>th</sup> passages were studied to estimate the population-doubling time. A suspension of  $1 \times 10^5$  cells was plated into 25-cm<sup>2</sup> culture flasks. The number of viable cells from three culture flasks per passage was measured with a Neubauer hemocytometer every 24 h for 8 d by trypan blue staining. The growth curve was plotted and the population doubling time of the CEK-Sq-1 cell line was calculated during the exponential growth phase of the cells and using online algorithm software provided at <http://www.doubling-time.com>.

### Establishment of the human experimental bone metastasis clone

The experimental animal study protocols were approved by the Shanghai Laboratory Animal Science Administration Commission of Shanghai Municipality. All BALB/c nu/nu nude mice (Shanghai Cancer Institute of Shanghai Jiaotong University, Shanghai, China) were maintained in a specific pathogen-free environment. Cells in the fifth passage were harvested from cell culture flasks and resuspended at  $1 \times 10^7$ /mL in phosphate buffered solution. Following this, 0.1 mL of the cell suspension was injected into the left cardiac ventricles of 8-wk-old male mice using 29 G needles. The mice were anesthetized as previously described<sup>[10]</sup>.

To begin with, the bone metastasis rate was 20% (2/10) for the fifth passage cells. The bone metastasis tumor clones were dissected and the cells cultured. On the second cycle of inoculation, about 40% (4/10) of the transplanted mice had bone metastasis. Starting with the fourth cycle, 90% of the transplanted mice had observable bone metastasis. Most of the bone metastasis sites were in the mandible, spine and four limbs; the other bone metastasis sites were the skull and ribs. The fourth cycle of the bone-seeking cells was named CEK-Sq-1BM.

### Bone metastatic imaging

BALB/c mice were deeply anesthetized with an intraperitoneal injection of 75-100 mg/kg thiopental. Bone metastasis was evaluated by *in vivo* imaging weekly micro-pinhole bone scintigraphy with <sup>99m</sup>Tc-methylene diphosphonate (<sup>99m</sup>Tc-MDP; Shanghai Syncor Pharmaceutical, Shanghai, China) starting 4 wk after inoculation. Static planar images of the entire skeleton were acquired 5-6 h after tail vein injection of 111 MBq (3 mCi), or 0.1 mL <sup>99m</sup>Tc-MDP on a GE Hawkeye 4 Infinia Functional Imaging Scanner (GE Medical Systems, Waukesha, WI, United States) with a pinhole collimator. The pinhole insert had been designed and built for obtaining ultra-high resolution images, with an aperture diameter of 1 mm. Radiography images were used as controls. Conventional radiographs were obtained with a Philips Optimus Bucky Diagnost TS X-ray System (Philips Healthcare, Eindhoven, The Netherlands). Bone metastases were determined using the radiograph tube voltage fixed at 40 kVp,

the current at 2 mA, and the exposure time at 3 s<sup>[10]</sup>.

### Micro PET/CT imaging

A high resolution, animal positron emission tomography/computed tomography (PET/CT) scanner (Inveon micro PET/CT, Siemens Preclinical Solution, Knoxville, TN, United States) was used to image the BALB/c nu/nu nude mice. For each imaging session, awake mice were injected with 0.15-0.2 mCi of <sup>18</sup>F-FLT, given tail vein injection. Each mouse was anesthetized with 5% isoflurane in an induction chamber. Afterwards, the mouse was placed in the scanner bed in the prone position with the long axis of the heart parallel and within the FOV of the scanner. During image acquisition, the mice were anesthetized with 1%-2% isoflurane gas delivered through a custom face mask.

All micro-PET images were reconstructed with the standard ordered-subset expectation maximization (OSEM) method. Reconstructed images were displayed in transverse, coronal and sagittal planes. A total of 512 sequential tomographic slices were displayed over the imaging object of interest with each slice measuring 0.11 mm in thickness, and assessed visually using transaxial, sagittal, and coronal displays. CT images were used for both attenuation correction of emission data and image fusion.

### Histological examination

Every tumor-bearing nude mouse was sacrificed with deep anesthesia 45 d after inoculation and cut into eight skeleton sites (mandible, spine and both scapula, humerus, femur) for histological diagnosis. Bone metastasis clones were observed by radionuclide scintigraphy and radiography, and the bony tissue was dissected and formalin soaked, decalcified, embedded in paraffin, cut in thin sections, and stained with hematoxylin and eosin (H&E). Each of the slides was examined independently by two pathology specialists.

### Real-time PCR

Total RNA was extracted from parental CEK-Sq-1 and CEK-Sq-1BM cells with TRIzol reagent (Gibco). Quantitative real-time reverse transcriptase-polymerase chain reaction (RT-PCR) was used to validate gene expressions of the bone metastasis cells. Reverse transcription was performed using the Reverse Transcriptase Kit (Promega, San Luis Obispo, CA, United States) following the manufacturer's instructions. We performed a set of real-time PCR assays with the approximation method using the  $\Delta\Delta CT$  method. In the  $\Delta\Delta CT$  method, GAPDH served as the endogenous control and the examined genes were *CDH1* (E-cadherin), *SERPINA1*, *SERPINE2*, *FN1*, *POU5F1* (OCT<sub>4</sub>) and *AR*. The quantitative real-time PCR was performed in triplicate using SYBR Green Mastermix (TaKaRa, Kyoto, Japan) on the ABI Prism 7900 Sequence Detection System (Applied Biosystems, Foster City, CA, United States). PCR conditions were 95 °C for 15 s, 45 cycles of 95 °C for 20 s, 60 °C for 20 s and 72 °C for 20 s. The PCR primer sequences are shown in Table 1.

**Table 1 Primers for real-time polymerase chain reaction**

Gene name	Forward primer	Reverse primer
<i>POU5F1</i>	GTAGGTTCTGAATCCCGAATG	TCTGCTTTGCATATCTCCTGAA
<i>FN1</i>	CTGCTGGGACTTCCTATGTGGT	GGTTTCCTCGATTATCCTTCTTG
<i>CDH1</i>	CTTCTGCTGACCTGCTGATG	GTCACACACGCTGACCTCTAAG
<i>SERPINE2</i>	TCAGCACCAAGACCATAGACAG	CGGATGAAAAACAGAAAAGGTC
<i>SRPINA1</i>	AACGATTACGTGGAGAAGGTA	GGTAAATGTAAGCTGGCAGACC
<i>AR</i>	ATTGAGCCAGGTGTAGTGTG	GGAGTTGACATTGGTGAAGGAT

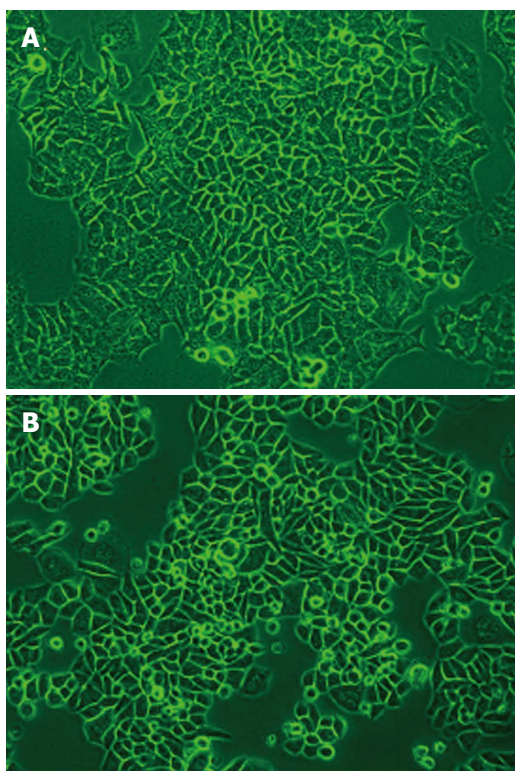


**Figure 1 Morphology of human esophageal squamous cell carcinoma cell line CEK-Sq-1.** A: First passage oncogenic cells (× 100); B: After four cycles, the bone-seeking subline CEK-Sq-1BM was harvested.

## RESULTS

### Morphologic characterization

The CEK-Sq-1 cells from the xenograft tumor were adherent and tended to form a monolayer with epithelial features. Many morphologically distinct populations were found, such as small rounded, polygonal and spindle cells. Such heterogeneous cell types were observed from the first-passage oncogenic cells in culture (Figure 1A). The morphology of the cells remained unchanged even after 40 passages. After four cycles *in vivo/in vitro*, the bone-seeking clone CEK-Sq-1BM was harvested (Figure 1B).

### Growth curve and doubling time

Figure 2 shows the growth curve and population doubling time of the established ESCC cell line; the population doubling was calculated from the growth curve. The analyzed cells were from the 7<sup>th</sup>, 24<sup>th</sup> and 40<sup>th</sup> passages. The population doubling time of the ESCC cells was

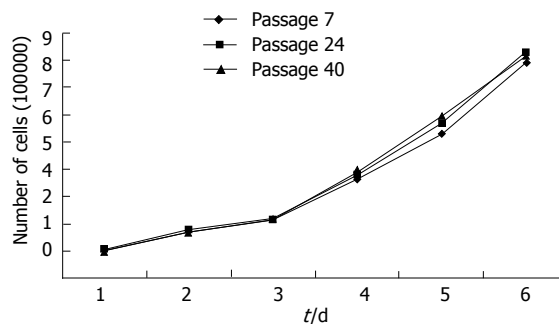


**Figure 2 Growth curve of the CEK-Sq-1 cell line at passages 7, 24 and 40.**

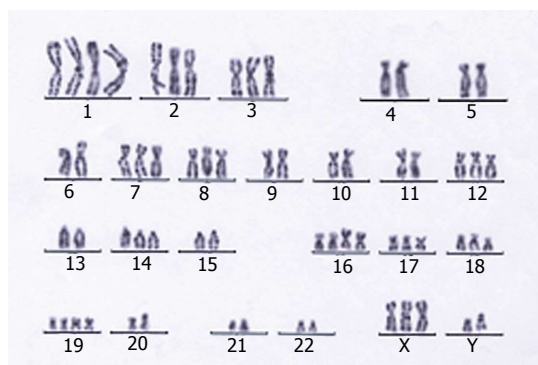


**Figure 3 Chromosomal imbalances of CEK-Sq-1 shows the DNA over-representation on chromosomes 1-3, 7, 8, 12, 14, 16-19, X and Y.**

about 46 h.

### Karyotype

Karyotypic study revealed both numerical and structural abnormalities in this ESCC cell line. The modal number of chromosomes ranged from 58 to 68, with a median of 64. Most of the analyzable metaphases were hypotriploid (Figure 3).

### Bone metastasis images

The bone metastasis lesions were detected by <sup>99m</sup>Tc-MDP micro-pinhole bone scintigraphy, X-ray, and micro-PET/CT. CEK-Sq-1BM was obtained after four cycles of the *in vivo/in vitro* repeat. The suspicious bone metastasis sites were scanned weekly under anesthesia 4 wk after inoculation of CEK-Sq-1 cells. The bone metastasis images of CEK-Sq-1BM mice were acquired by X-rays, micro-pinhole bone scintigraphy and micro-PET/CT (Figures 4 and 5). The whole-body X-ray image showed osteo-

**Table 2 Sensitivity, specificity and accuracy with different techniques for pathology using  $\chi^2$  test**

	Micro-pinhole BS (n = 7)		X-ray (n = 7)		Micro-PET/CT (n = 7)	
	+	-	+	-	+	-
Histology +	18	2	6	13	16	3
-	4	32	0	37	4	33

PET/CT: Positron emission tomography/computed tomography.

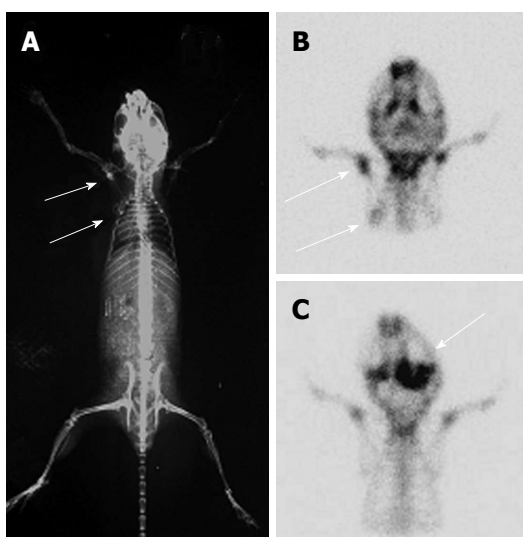


**Figure 4 Whole-body X-ray and micro-pinhole bone scintigraphy images of experimental bone metastasis in mice.** A: X-ray image, upper arrow indicates the hot spot of the left humeral osteoblastic metastatic lesion, and the lower arrow indicates the cold spot of the left scapular osteolytic metastatic lesion and circle around the osteogenic reaction; B: Micro-pinhole bone scintigraphy images of the same mouse in the POST position. The osteoblastic metastatic lesion (upper arrow) showed greater accumulation of  $^{99m}\text{Tc}$ -methylene diphosphonate ( $^{99m}\text{Tc}$ -MDP), and the osteolytic lesion (lower arrow) combined with osteogenic reaction showed less; C: The arrow indicates a mandibular lesion in another mouse with accumulation of  $^{99m}\text{Tc}$ -MDP.

blastic metastasis concurrent with osteolytic in a CEK-Sq-1 BM mouse at 6-8 wk (Figure 4A). The difference of osteoblastic and osteolytic metastasis presented in the same mouse by micro-pinhole bone scintigraphy (Figure 4B). The mandibular lesions of another model mouse accumulated  $^{99m}\text{Tc}$ -MDP (Figure 4C). All of the suspicious bone metastasis sites were evaluated by histological examination after the mice were sacrificed, and the sensitivity, specificity and accuracy of micro-pinhole bone scintigraphy, X-ray, and micro-PET/CT imaging examinations were: 89.66%/32%/80%, 88.2%/100%/89.2%, and 88.75%/77.5%/87.5%, respectively (Table 2).

**Histological examination**

Figure 6 shows the histological examination of mandible (A) and lumbar vertebrae (B), confirming the bone metastasis sites (stained with H&E, magnification  $\times 100$  and  $\times 200$ , respectively).

**Real-time PCR analysis of CEK-Sq-1 and CEK-Sq-1BM**

Ratios of CEK-Sq-1BM compared to CEK-Sq-1. Can-

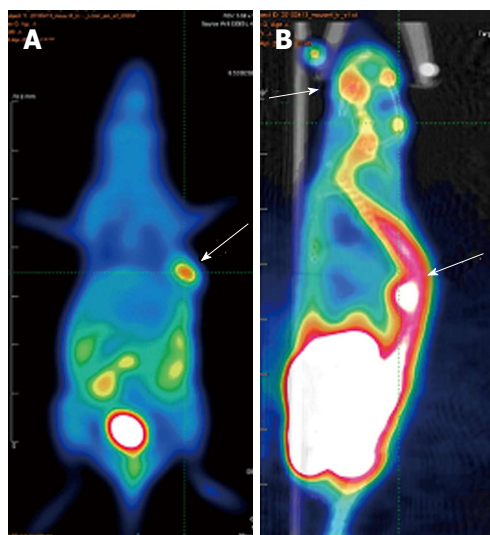


**Figure 5  $^{18}\text{F}$ -FLT micro-PET/CT images of CEK-Sq-1MB mouse.** A: Arrow indicates  $^{18}\text{F}$ -FLT uptake positivity in the cells ( $2 \times 10^6$ ) injected subcutaneously into the left lateral subcutis of the mouse for 3 wk; B: Arrows indicate the mandibular and thoracic vertebral metastatic lesions of the cells after intracardiac injection in mice for 4 wk.

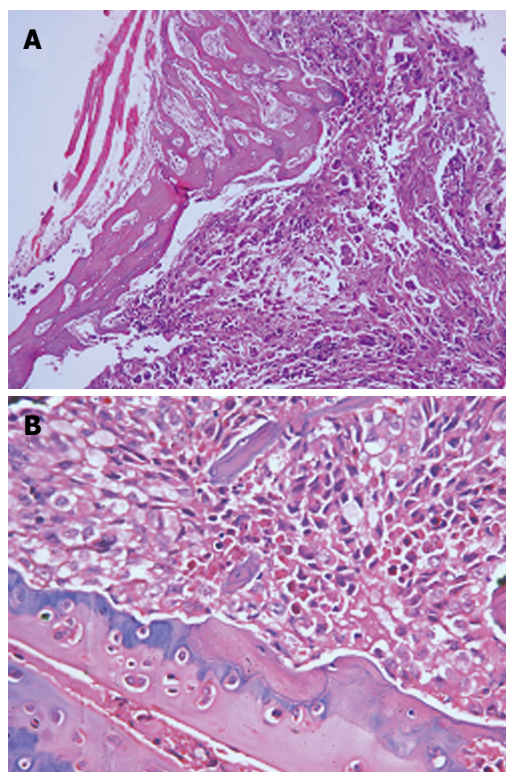


**Figure 6 Histological features of the the mandibular (A) (hematoxylin and eosin,  $\times 100$ ) and lumbar vertebral (B) (hematoxylin and eosin,  $\times 200$ ) metastatic lesions.**

cer invasion and metastasis are complex multistep processes<sup>[11]</sup>. Cancer cells invasion into blood vessels initiates metastasis, and the vessels also provide the routes for systemic spread of cancer cells<sup>[12]</sup>. Low apoptosis leads to clonal expansion and continuous selection of progressively more malignant cell populations<sup>[13]</sup>. Cell-cell adhesion plays an important role in metastasis too<sup>[14]</sup>. Thus, to

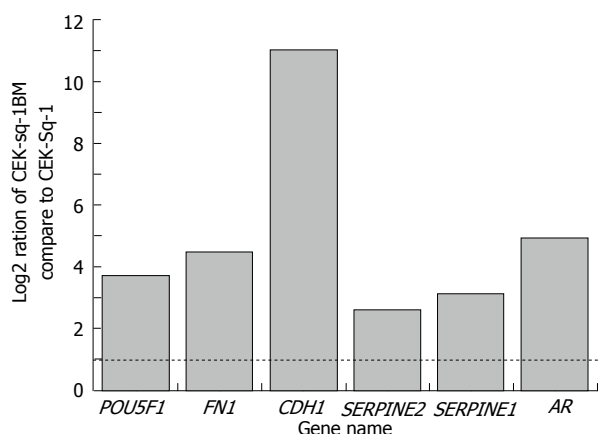


**Figure 7** Expression changes of genes determined in CEK-Sq-1BM cells compared with CEK-Sq-1 cells.

examine that CEK-Sq-1BM had metastasis capacity compared with that of the CEK-Sq-1, we performed real-time PCR to detect changes in gene expression. Genes associated with cell adhesion molecules, such as *CDH1*, *SERPINA1*, *SERPINE2*, *FN1*, *POU5F1* and *AR* were examined.

As shown in Figure 7, the expression of *CDH1*, *AR*, *FN1* and *POU5F1* was increased in CEK-Sq-1BM compared to that in CEK-Sq-1 cells, while the expression of *SERPINE2* and *SERPINA1* was moderately increased. We selected these genes that were overexpressed in cancer metastasis by real-time PCR analysis, and confirmed their high expression in CEK-Sq-1BM cells. This indicated that the clone did indeed have metastatic capacity compared to its parental CEK-Sq-1 cells.

## DISCUSSION

EC is one of the least studied and deadliest cancers worldwide; the treatment of EC, especially advanced stage, remains challenging. Therefore, cell lines and human xenograft models that accurately mimic human EC are needed to elucidate the biological characteristics of these tumors. However, the available and useful cell lines and animal models of ESCC remain limited, especially for metastatic models.

The first melanoma bone metastasis animal model was established early in 1988<sup>[15]</sup>. Breast cancer<sup>[16]</sup>, prostate cancer<sup>[17]</sup>, and small cell lung cancer bone metastasis models<sup>[18]</sup> were then successfully established. However, to the best of our knowledge, no experimental EC bone metastasis models have been reported so far. One of the important reasons may be the lack of a highly potent bone metastasis cell line. Second, the modeling methods are labor intensive, involving anesthesia, cancer cell injection into the left cardiac ventricle of mice, and then resuscitation. Third, <sup>99m</sup>Tc-MDP micro-pinhole bone scintigraphy and micro-SPECT/CT, which can detect osteoblastic metastases with great sensitivity, have only recently been developed. Fourth, <sup>18</sup>F-fluoride micro-PET/CT scans

mainly detect osteolytic metastases, which is also the limitation of X-rays, which is the most commonly used method to search for bone metastasis, requiring about 30%-75% reduction in bone density to visualize a metastasis<sup>[19]</sup>.

During the lifespan of a tumor-bearing mouse, which is generally 30-60 d, the metastasis sites may not be observed by X-rays because of limited bone density reduction. For detecting bone metastasis with bone scintigraphy, at least a 5%-10% change in the ratio of lesion to normal bone is required to detect an abnormality. It has been estimated that bone scintigraphy can detect malignant bone lesions 2-18 mo earlier than plain radiography, and bone scintigraphy sensitivities in detecting bone metastases vary between 62% and 100% with specificity of 78%-100%. This is because the alteration in osteoblastic action and/or blood supply occurs at an earlier stage than the difference in bone density needed to produce a radiographic change<sup>[20,21]</sup>. For bone metastasis examination, bone scintigraphy could have a similar sensitivity and specificity to PET/CT, but with a relative economic advantage leading to more common use in clinical and experimental research<sup>[22]</sup>.

We established an experimental lung adenocarcinoma bone metastasis cell line and mouse model in 2009 with a gamma camera using <sup>99m</sup>Tc-MDP micro-pinhole bone scintigraphy, which was the first and is still the only lung adenocarcinoma model<sup>[10]</sup>. The same technique was used to establish this new EC cell line with high bone metastasis potency. All of the suspicious bone metastasis sites were confirmed by pathological examination, with a sensitivity of 89.66% and a specificity of 88.2%, which demonstrates the advantage of micro-pinhole bone scintigraphy over X-rays.

The formation of bony metastases is a multi-gene, multi-step synergistic process that includes intravasation of tumor cells from the primary site into the bloodstream, survival while in the circulation, adhesion to endothelial cells within the target organ, and extravasation from the bloodstream into the surrounding tissue<sup>[23]</sup> or marrow cavity. Cell-cell adhesion molecules *SERPINE2* and *SERPINA1* have been proven to play important roles in the increased metastasis and invasion potency of lung adenocarcinoma, pancreatic and colorectal tumors<sup>[10,24,25]</sup>. *FN1*, a cellular adhesion factor, is associated with tumor metastasis and forms a highly interactive network in ESCC<sup>[26]</sup>. In renal cancer<sup>[27]</sup>, melanoma<sup>[28]</sup> and non-small cell lung cancer<sup>[29]</sup>, *FN1* is required for cell invasion and metastasis. *CDH1* is a 120-kDa transmembrane glycoprotein belonging to the Super family of Ca<sup>2+</sup>-dependent cell adhesion molecules and its role remains controversial in malignant progression<sup>[30,31]</sup>. In addition, E-cadherin is one of the cell surface markers of human embryonic stem cells (hESCs)<sup>[32]</sup>. The bone metastasis and primary tissue sections of prostate cancer were stained by immunohistochemistry using specific antibody to *CDH1*, which showed *CDH1* overexpression in bone metastasis<sup>[33]</sup>. *CDH1* upregulation may be related to osteolytic or

mixed bone metastasis. POU5F1, a member of the POU (Pit-Oct-Unc) family of transcriptional factors, is essential for maintenance of the stem character in hESCs. The expression of POU5F1 has been proven to increase the risk of metastasis and markedly enhance resistance to cytotoxic agents<sup>[34]</sup>. These hESC markers (E-cadherin and OCT4) may promote the initiation, progression, and differentiation of human cancers. Androgen receptors (ARs) are probably of importance during all phases of prostate cancer growth and assessment of breast cancer prognosis, but their role in bone metastases is largely unexplored<sup>[35,36]</sup>.

In conclusion, we established a new ESCC cell line, CEK-Sq-1, from ESCC tissue, which had high bone metastatic potency. To the best of our knowledge, no investigations have been reported of cell lines and bone metastasis animal models with EC tumors. This newly established cell line and animal model may provide a useful tool for the study of the pathogenesis of EC.

## ACKNOWLEDGMENTS

We thank Chengmo Zhu, MD; Jixiao Ma, MD; Meiping Shi, MD; Jiuxian Feng, MD; Ning Zheng, PhD; Yifeng Jiang, MD; Zhichun Zheng, MD for scientific suggestions and technical help. We thank the technicians of radiology department at Shanghai Chest Hospital of Shanghai Jiaotong University for their supports.

## COMMENTS

### Background

Esophageal cancer (EC) is among the top six leading causes of death from recurrence or metastasis, with a 5-year survival rate as low as 16% in the United States. In China, the situation is even worse, especially in the north. The most common metastatic sites of EC are lung, liver and bone. To improve survival for EC patients, a better understanding of the cellular and molecular carcinogenesis, especially of the mechanism of metastasis, is needed, but a bone metastasis model is lacking. The authors established a new human EC cell line (CEK-Sq-1) and its clone with a high bone-seeking tendency. Their morphological and biological characteristics and tumorigenicity *in vivo* were described in this experimental study. The results may provide a useful model for *in vitro* and *in vivo* cellular and molecular research.

### Research frontiers

The cells came from oncogenic tissue in a BALB/c nu/nu immunodeficient mouse and from a surgical specimen from a 61-year-old male Chinese patient with esophageal squamous cell carcinoma (ESCC). The oncogenic cells were injected into the left cardiac ventricle of immunodeficient mice. The bone metastatic lesions of tumor-bearing mice were detected by <sup>99m</sup>Tc-methylene diphosphonate (<sup>99m</sup>Tc-MDP) scintigraphy, micro-positron emission tomography/computed tomography and X-rays, and were resected from the mice under deep anesthesia. The bone metastatic cells in the lesions were used for culture and repeated intracardiac inoculation. This *in vivo/in vitro* study was repeated four times. All of the suspicious bone sites were confirmed by pathology. Real-time polymerase chain reaction was used to compare the gene expression in the parental cells (CEK-Sq-1) and in the bone metastatic clone (CEK-Sq-1BM).

### Innovations and breakthroughs

A novel ESCC cell line (CEK-Sq-1) and its bone metastasis clone (CEK-Sq-1BM) were established from a Chinese patient by molecular imaging. Some differences in gene expression and the characteristics of the bone metastatic lesions were revealed, which could form the basis for further research into ESCC.

### Applications

This study established a new research method that could be used for studies on ESCC, including tumor cells, animal models and tumor markers.

## Peer review

The authors first showed the morphology of the newly established ESCC cell line and molecular imaging of its bone-seeking clone. Most importantly, the authors showed the karyotype of this cell line, identified the type of bone metastasis and hypothesized markers, which is especially important.

## REFERENCES

- 1 Jemal A, Center MM, DeSantis C, Ward EM. Global patterns of cancer incidence and mortality rates and trends. *Cancer Epidemiol Biomarkers Prev* 2010; **19**: 1893-1907 [PMID: 20647400 DOI: 10.1158/1055-9965.EPI-10-0437]
- 2 Jemal A, Siegel R, Ward E, Hao Y, Xu J, Thun MJ. Cancer statistics, 2009. *CA Cancer J Clin* 2009; **59**: 225-249 [PMID: 19474385 DOI: 10.3322/caac.20006]
- 3 Siegel R, Naishadham D, Jemal A. Cancer statistics, 2012. *CA Cancer J Clin* 2012; **62**: 10-29 [PMID: 22237781 DOI: 10.3322/caac.20138]
- 4 Yang L, Parkin DM, Li L, Chen Y. Time trends in cancer mortality in China: 1987-1999. *Int J Cancer* 2003; **106**: 771-783 [PMID: 12866039 DOI: 10.1002/ijc.11300]
- 5 Shimada Y, Imamura M, Wagata T, Yamaguchi N, Tobe T. Characterization of 21 newly established esophageal cancer cell lines. *Cancer* 1992; **69**: 277-284 [PMID: 1728357]
- 6 Zhang QB, Gao YP, He JT, Zhang TT, Lin P, Zhang J, Wang XJ. Establishment of a novel human esophageal squamous cell carcinoma cell line (ESC-410) and its partial biological characterization. *Dis Esophagus* 2011; **24**: 120-126 [PMID: 20819098 DOI: 10.1111/j.1442-2050.2010.01106.x]
- 7 Hu YC, Lam KY, Law SY, Wan TS, Ma ES, Kwong YL, Chan LC, Wong J, Srivastava G. Establishment, characterization, karyotyping, and comparative genomic hybridization analysis of HKESC-2 and HKESC-3: two newly established human esophageal squamous cell carcinoma cell lines. *Cancer Genet Cytogenet* 2002; **135**: 120-127 [PMID: 12127396 DOI: 10.1016/S0165-4608(01)00580-5]
- 8 Sarbia M, Bösing N, Hildebrandt B, Koldovsky P, Gerharz CD, Gabbert HE. Characterization of two newly established cell lines derived from squamous cell carcinomas of the oesophagus. *Anticancer Res* 1997; **17**: 2185-2192 [PMID: 9216685]
- 9 Mok CH, Chew EC, Riches DJ, Lee JC, Huang DP, Hadjis C, Crofts TJ. Biological characteristics of a newly established human oesophageal carcinoma cell line. *Anticancer Res* 1987; **7**: 409-415 [PMID: 3631894]
- 10 Yang S, Dong Q, Yao M, Shi M, Ye J, Zhao L, Su J, Gu W, Xie W, Wang K, Du Y, Li Y, Huang Y. Establishment of an experimental human lung adenocarcinoma cell line SPC-A-1BM with high bone metastases potency by (<sup>99m</sup>Tc)-MDP bone scintigraphy. *Nucl Med Biol* 2009; **36**: 313-321 [PMID: 19324277 DOI: 10.1016/j.nucmedbio.2008.12.007]
- 11 Liotta LA, Wewer U, Rao NC, Schiffmann E, Stracke M, Guirguis R, Thorgerirsson U, Muschel R, Sobel M. Biochemical mechanisms of tumor invasion and metastases. *Prog Clin Biol Res* 1988; **256**: 3-16 [PMID: 2835781]
- 12 O'Reilly MS, Holmgren L, Shing Y, Chen C, Rosenthal RA, Moses M, Lane WS, Cao Y, Sage EH, Folkman J. Angiostatin: a novel angiogenesis inhibitor that mediates the suppression of metastases by a Lewis lung carcinoma. *Cell* 1994; **79**: 315-328 [PMID: 7525077 DOI: 10.1016/0092-8674(94)90200-3]
- 13 Reya T, Morrison SJ, Clarke MF, Weissman IL. Stem cells, cancer, and cancer stem cells. *Nature* 2001; **414**: 105-111 [PMID: 11689955 DOI: 10.1038/35102167]
- 14 Mareel M, Leroy A. Clinical, cellular, and molecular aspects of cancer invasion. *Physiol Rev* 2003; **83**: 337-376 [PMID: 12663862]
- 15 Arguello F, Baggs RB, Frantz CN. A murine model of experimental metastasis to bone and bone marrow. *Cancer Res* 1988; **48**: 6876-6881 [PMID: 3180096]
- 16 Sasaki A, Boyce BF, Story B, Wright KR, Chapman M, Boyce

- R, Mundy GR, Yoneda T. Bisphosphonate risedronate reduces metastatic human breast cancer burden in bone in nude mice. *Cancer Res* 1995; **55**: 3551-3557 [PMID: 7627963]
- 17 **Rabbani SA**, Harakidas P, Bowlin T, Attardo G. Effect of nucleoside analogue BCH-4556 on prostate cancer growth and metastases in vitro and in vivo. *Cancer Res* 1998; **58**: 3461-3465 [PMID: 9699681]
- 18 **Miki T**, Yano S, Hanibuchi M, Kanematsu T, Muguruma H, Sone S. Parathyroid hormone-related protein (PTHrP) is responsible for production of bone metastasis, but not visceral metastasis, by human small cell lung cancer SBC-5 cells in natural killer cell-depleted SCID mice. *Int J Cancer* 2004; **108**: 511-515 [PMID: 14696114 DOI: 10.1002/ijc.11586]
- 19 **Even-Sapir E**. Imaging of malignant bone involvement by morphologic, scintigraphic, and hybrid modalities. *J Nucl Med* 2005; **46**: 1356-1367 [PMID: 16085595]
- 20 **Blake GM**, Park-Holohan SJ, Cook GJ, Fogelman I. Quantitative studies of bone with the use of 18F-fluoride and 99mTc-methylene diphosphonate. *Semin Nucl Med* 2001; **31**: 28-49 [PMID: 11200203 DOI: 10.1053/snuc.2001.18742]
- 21 **Rybak LD**, Rosenthal DI. Radiological imaging for the diagnosis of bone metastases. *Q J Nucl Med* 2001; **45**: 53-64 [PMID: 11456376]
- 22 **Virk MS**, Petrigliano FA, Liu NQ, Chatziioannou AF, Stout D, Kang CO, Dougall WC, Lieberman JR. Influence of simultaneous targeting of the bone morphogenetic protein pathway and RANK/RANKL axis in osteolytic prostate cancer lesion in bone. *Bone* 2009; **44**: 160-167 [PMID: 18929692 DOI: 10.1016/j.bone.2008.09.009]
- 23 **Chambers AF**, Groom AC, MacDonald IC. Dissemination and growth of cancer cells in metastatic sites. *Nat Rev Cancer* 2002; **2**: 563-572 [PMID: 12154349 DOI: 10.1038/nrc865]
- 24 **Buchholz M**, Biebl A, Neesse A, Wagner M, Iwamura T, Leder G, Adler G, Gress TM. SERPINE2 (protease nexin I) promotes extracellular matrix production and local invasion of pancreatic tumors in vivo. *Cancer Res* 2003; **63**: 4945-4951 [PMID: 12941819]
- 25 **Bergeron S**, Lemieux E, Durand V, Cagnol S, Carrier JC, Lussier JG, Boucher MJ, Rivard N. The serine protease inhibitor serpinE2 is a novel target of ERK signaling involved in human colorectal tumorigenesis. *Mol Cancer* 2010; **9**: 271 [PMID: 20942929 DOI: 10.1186/1476-4598-9-271]
- 26 **Wong FH**, Huang CY, Su LJ, Wu YC, Lin YS, Hsia JY, Tsai HT, Lee SA, Lin CH, Tzeng CH, Chen PM, Chen YJ, Liang SC, Lai JM, Yen CC. Combination of microarray profiling and protein-protein interaction databases delineates the minimal discriminators as a metastasis network for esophageal squamous cell carcinoma. *Int J Oncol* 2009; **34**: 117-128 [PMID: 19082484]
- 27 **Waalkes S**, Atschekzei F, Kramer MW, Hennenlotter J, Vetter G, Becker JU, Stenzl A, Merseburger AS, Schrader AJ, Kuczyk MA, Serth J. Fibronectin 1 mRNA expression correlates with advanced disease in renal cancer. *BMC Cancer* 2010; **10**: 503 [PMID: 20860816 DOI: 10.1186/1471-2407-10-503]
- 28 **Bittner M**, Meltzer P, Chen Y, Jiang Y, Seftor E, Hendrix M, Radmacher M, Simon R, Yakhini Z, Ben-Dor A, Sampas N, Dougherty E, Wang E, Marincola F, Gooden C, Lueders J, Glatfelter A, Pollock P, Carpten J, Gillanders E, Leja D, Dietrich K, Beaudry C, Berens M, Alberts D, Sondak V. Molecular classification of cutaneous malignant melanoma by gene expression profiling. *Nature* 2000; **406**: 536-540 [PMID: 10952317 DOI: 10.1038/35020115]
- 29 **Han S**, Ritzenthaler JD, Sitaraman SV, Roman J. Fibronectin increases matrix metalloproteinase 9 expression through activation of c-Fos *via* extracellular-regulated kinase and phosphatidylinositol 3-kinase pathways in human lung carcinoma cells. *J Biol Chem* 2006; **281**: 29614-29624 [PMID: 16882662 DOI: 10.1074/jbc.M604013200]
- 30 **Chung Y**, Law S, Kwong DL, Luk JM. Serum soluble E-cadherin is a potential prognostic marker in esophageal squamous cell carcinoma. *Dis Esophagus* 2011; **24**: 49-55 [PMID: 20807231 DOI: 10.1111/j.1442-2050.2010.01093.x]
- 31 **Bae KM**, Parker NN, Dai Y, Vieweg J, Siemann DW. E-cadherin plasticity in prostate cancer stem cell invasion. *Am J Cancer Res* 2011; **1**: 71-84 [PMID: 21968440]
- 32 **Kolle G**, Ho M, Zhou Q, Chy HS, Krishnan K, Cloonan N, Bertonecello I, Laslett AL, Grimmond SM. Identification of human embryonic stem cell surface markers by combined membrane-polysome translation state array analysis and immunotranscriptional profiling. *Stem Cells* 2009; **27**: 2446-2456 [PMID: 19650036 DOI: 10.1002/stem.182]
- 33 **Sethi S**, Macoska J, Chen W, Sarkar FH. Molecular signature of epithelial-mesenchymal transition (EMT) in human prostate cancer bone metastasis. *Am J Transl Res* 2010; **3**: 90-99 [PMID: 21139809]
- 34 **Zhang X**, Han B, Huang J, Zheng B, Geng Q, Aziz F, Dong Q. Prognostic significance of OCT4 expression in adenocarcinoma of the lung. *Jpn J Clin Oncol* 2010; **40**: 961-966 [PMID: 20462980 DOI: 10.1093/jjco/hyq066]
- 35 **Crnalic S**, Hörnberg E, Wikström P, Lerner UH, Tieva A, Svensson O, Widmark A, Bergh A. Nuclear androgen receptor staining in bone metastases is related to a poor outcome in prostate cancer patients. *Endocr Relat Cancer* 2010; **17**: 885-895 [PMID: 20688881 DOI: 10.1677/ERC-10-0059]
- 36 **Ni M**, Chen Y, Lim E, Wimberly H, Bailey ST, Imai Y, Rimm DL, Liu XS, Brown M. Targeting androgen receptor in estrogen receptor-negative breast cancer. *Cancer Cell* 2011; **20**: 119-131 [PMID: 21741601 DOI: 10.1016/j.ccr.2011.05.026]

P- Reviewer: Xu XC S- Editor: Wen LL  
L- Editor: Kerr C E- Editor: Wu HL





百世登

**Baishideng**®

Published by **Baishideng Publishing Group Co., Limited**

Flat C, 23/F., Lucky Plaza,

315-321 Lockhart Road, Wan Chai, Hong Kong, China

Fax: +852-65557188

Telephone: +852-31779906

E-mail: [bpgoffice@wjgnet.com](mailto:bpgoffice@wjgnet.com)

<http://www.wjgnet.com>



ISSN 1007-9327



9 771007 932045